SLAC-PUB-2729
April 1981
(N)

OBSERVATION OF NEW RESONANCE STRUCTURE IN THE NATURAL SPIN PARITY STRANGE MESON SYSTEM*

(SLAC-Carleton-NRC Canada Collaboration)†

Blair N. Ratcliff
Stanford Linear Accelerator Center
Stanford University, Stanford, California 94305

ABSTRACT

New data from the LASS spectrometer are presented on the reaction $K^-p \rightarrow K^-\pi^+n$. An energy independent partial wave analysis of this data yields unique $K^-\pi^+$ elastic scattering partial wave amplitudes in the invariant mass region from 0.7 GeV to 1.8 GeV, and two distinguishable sets of amplitudes between 1.8 GeV and 2.3 GeV. These amplitudes confirm all of the well known $K\pi$ resonances, and display clear evidence for new resonance structure in the S, P and G waves in the mass region above 1.6 GeV.

* Work supported by the Department of Energy, contract DE-AC03-76SF00515.

† D. Aston, R. Carnegie, W. Dunwoodie, S. Durkin, P. Estabrooks, T. Fieguth, R. J. Hemingway, A. Honma, D. Hutchinson, W. B. Johnson, P. Kunz, T. Lasinski, D. W. G. S. Leith, L. Levinson, R. McKee, A. McPherson, W. T. Meyer, G. Oakham, B. N. Ratcliff, R. Richter, S. Shapiro, R. Stroynowski, S. Suzuki, S. Williams, J. Va'Vra.

(Invited talk presented at the XVIth Rencontre de Moriond: Nonperturbative QCD: Theory and Experiment, Les Arcs, France, March 15-27, 1981.)

At the present time, we are engaged in a systematic study of Kp interactions at 11 GeV/c using the LASS spectrometer at SLAC. Broadly stated, the physics goals of this program are to provide a "great leap forward" in our understanding of the strange (e.g., $s\bar{u}$), and strangeonium ($s\bar{s}$) mesons, and of the strangeness -2 and -3 hyperons (e.g., ssu). Even though our general understanding of the hadron spectrum has improved dramatically during the last decade, these areas remain poorly understood. This is largely because nature provides us with no stable meson or strange baryon targets, so that these areas must be studied in production experiments.

The experimental program consists of two separate experiments. In the first, we triggered on essentially the total inelastic cross section and attained a sensitivity of about 1000 ev/μb for K^-p interactions. This experiment was run in 1978 and provides the data sample on which this talk is based. We are presently extending this data sample by a factor of over five in a sequel experiment which uses both K^+ and K^- beams.

The scope of the experimental program is clearly very broad, and I can only discuss a small portion of it here. Today, I would like to focus on our recently completed energy independent partial wave analysis of the $K\pi$ system from the reaction

$$K^-p \rightarrow K^-\pi^+n \qquad (1)$$

at small values of momentum transfer. This reaction is dominated by π exchange, and historically has been an important source of information on $K\pi$ elastic scattering, and the natural spin-parity strange mesons.[1] In a previous analysis of the $K\pi$ system using reaction (1) and several other π exchange dominated reactions at 13 GeV, ($K^+p \rightarrow K^+\pi^+n$, $K^-p \rightarrow K^-\pi^-\Delta^{++}$, $K^+p \rightarrow K^+\pi^-\Delta^{++}$) Estabrooks et al.[2] presented clear evidence for the $J^P = 0^+\kappa(1500)$, as well as evidence for P wave resonance structure in the 1.65 GeV region in two out of four solutions. That analysis was restricted to $K\pi$ masses below 1.8 GeV. In this talk, we present a PWA of new 11 GeV data on reaction (1) which extends the measurements of $K^-\pi^+$ elastic scattering partial waves up to a mass of 2.3 GeV. These partial waves confirm the results of Estabrooks et al.[2] in the low mass region ($M_{K\pi} < 1600$ MeV) while clearly displaying additional resonance structure at higher masses.

Events corresponding to reaction (1) were selected from the charge-zero two-prong sample by requiring the missing mass opposite the outgoing $K^-\pi^+$ system to lie in the range from 0.45 GeV to 1.05 GeV. Events ambiguous with elastic K^-p events and K^o decay events were explicitly rejected. The final $K^-p \rightarrow K^-\pi^+n$ data sample consisted of ~43,000 events in the $K\pi$ invariant mass range from 0.7 GeV to 2.3 GeV, and the small momentum transfer region, $|t'| < 0.2$ GeV^2. With these cuts, the background to reaction (1) was estimated to be $4 \pm 4\%$.

A maximum likelihood fitting procedure was used to correct the raw data for effects due to spectrometer acceptance, event selection criteria, and other factors. This procedure yields t-channel acceptance corrected Kπ angular moments as a function of the Kπ invariant mass and t'. In these fits the number of L and M moments was limited ($L < L_{max}$, $M < M_{max}$) to the minimum number required to describe the data in each mass region. Because reaction (1) is dominated by π exchange the prominent (M) moments are those with $M = 0$. These are shown in Fig. 1 as a function of $M_{K\pi}$. The most prominent structures in the even L moments are due to the leading K^* resonances (the $J^P = 1^- K^*(892)$, $2^+ K^*(1430)$, $3^- K^*(1780)$, and the newly discovered $J^P = 4^+ K^*(2090)$ [3]) while clear interference effects can be seen in the odd angular moments.

We have performed an energy independent Kπ scattering partial wave analysis using these spherical harmonic moments with an additional cut on the lower vertex (nπ) mass. The Kπ scattering analysis method used is identical to that employed in the previous PWA of the 13 GeV data performed by this group.[2] By extrapolating the π exchange contribution to the pole, this analysis determines the magnitudes and relative phases of the $K\pi \rightarrow K\pi$ scattering partial waves (one overall phase cannot be determine). Below 1.2 GeV the S and P waves are known to be elastic,[2] so the imposition of elastic unitarity on the S and P waves is sufficient to fix the overall phase. In the inelastic region above 1.2 GeV we fix the phase of the leading K^* resonance in each mass region near to the Breit-Wigner phase of the associated resonance as is shown in Fig. 3.

There are also discrete ambiguities inherent in any pseudoscalar-pseudoscalar amplitude analysis. These ambiguities are most readily apparent as ambiguities in the sign of the imaginary part of the amplitude zeros described by Barrelet.[4] Requiring the solutions to be smooth, it is possible to switch from one solution to another only when the imaginary part of a particular Barrelet zero approaches zero. Since the Wigner condition combined with the existence of leading resonances requires all of the $\mathrm{Im}(Z_i)$ to enter our solutions negatively, elastic unitarity leads to a unique solution below 1.20 GeV. It is seen in Fig. 2 that ambiguities do not arise until $\mathrm{Im}(Z_3)$ approaches zero in the 1.86 GeV region. In the region between 1.9 and 2.0 GeV, $\mathrm{Im}(Z_1)$ is also nearly zero. Thus, we extract one unique solution below 1.86 GeV, two distinct solutions in the region between 1.86 and 2.02 GeV, and four solutions above 2.02 GeV. The definitions of these four solutions in terms of the signs of the imaginary parts of the amplitude zeros in each mass region can be found in Table I.

The $K^-\pi^+$ partial wave magnitudes and phases are shown in Fig. 3. In general, these results are consistent with, but of higher statistical significance than previous measurements, particularly in the region above the $K^*(1430)$. The four high mass solutions presented actually fall into only two physically distinct

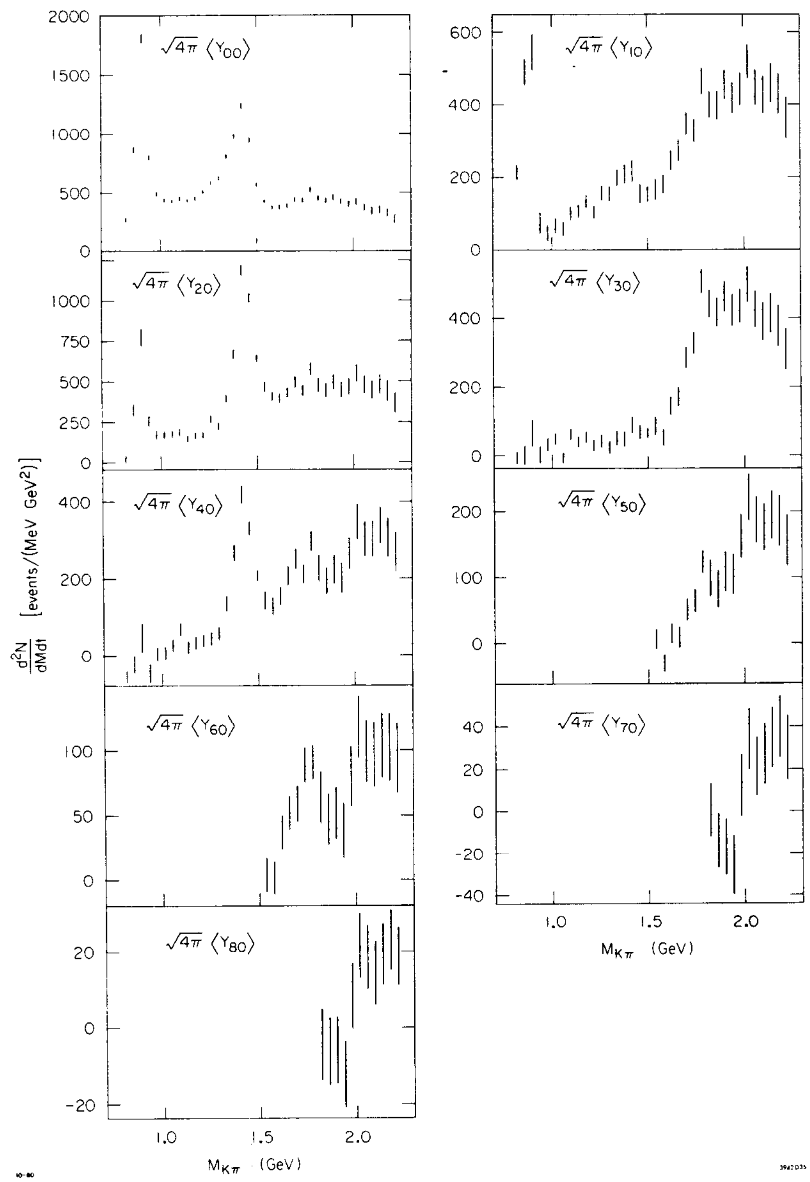

Fig. 1. The final $M = 0$ acceptance corrected angular moments as a function of mass. These moments are calculated in 40 MeV bins below 1.8 GeV, and 80 MeV overlapping bins above this mass. The moments have been divided by the mass bin and t' bin width.

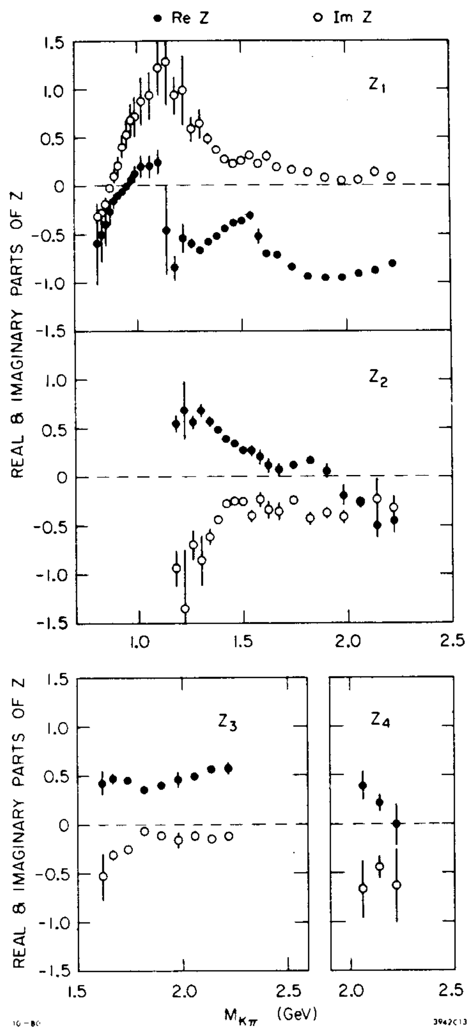

Fig. 2. The amplitude (Barrelet) zeros as a function of mass.

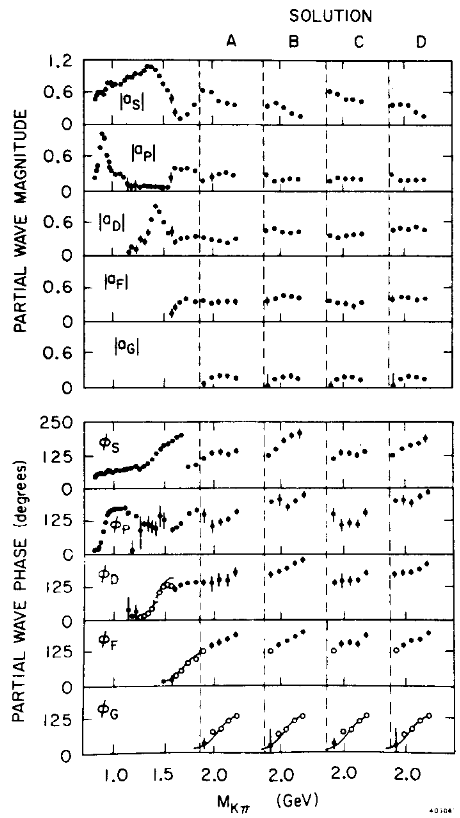

Fig. 3. These data were fit in 20 MeV bins below 1.06 GeV, 40 MeV bins from 1.6 GeV to 1.67 GeV, and 80 MeV bins above 1.67 GeV. The solid line represents the phase predicted by a simple Breit-Wigner fit to the leading resonance in the given mass region. The actual phase in each mass region has been fixed to the phase represented by the symbol o. Where error bars are not shown the size of the points plotted is larger than the statistical error associated with the point.

TABLE I

The Barrelet Zero Solution Classifications

Solution \ Mass (GeV)	1.30 – 1.86			1.86 – 2.02				2.02 – 2.30			
	z_1	z_2	z_3	z_1	z_2	z_3	z_4	z_1	z_2	z_3	z_4
A	+	–	–	+	–	+	–	–	–	+	–
B	+	–	–	+	–	–	–	–	–	–	–
C	+	–	–	+	–	+	–	+	–	+	–
D	+	–	–	+	–	–	–	+	–	–	–

groups (A,C) and (B,D) based primarily on the behavior of the S and P waves. The behavior of the D,F and G waves are essentially independent of the solution. In the ambiguous region the S wave shows relatively similar magnitude peaks coupled with rapid phase motion in all four solutions. Only the P wave above 2 GeV differs substantially between the two solution sets.

All solutions display the leading $J^P = 1^-, 2^+, 3^-$ and 4^+ resonances clearly. Additional resonance structure is also seen in the S and P wave solutions. This structure is more easily viewed in the Argand diagrams of Fig. 4 which show the two physically distinct solutions (A,C). In these diagrams, significant departures from the unitary circle can be seen in the S wave solutions at low mass. These departures are due to the fact that the partial waves presented are the sum of the different isospin parts ($a_L = a_L^{1/2} + \frac{1}{2} a_L^{3/2}$). The 3/2 component has been well measured up to 1.6 GeV and contains no significant waves other than the S wave. Above 1.6 GeV, little $I = 3/2$ information exists. In the S wave plots of Fig. 4, the dotted lines represent our S wave solutions with the isospin 3/2 component subtracted up to 1.6 GeV using the parameterization of Ref. 1. The resulting S wave remains within the unitary circle.

The leading K^* resonances are readily apparent as counter clockwise loops in the appropriate Argand diagrams. In particular, the new $J^P = 4^+ K^*(2090)$ is indicated by the G wave loop in the 2.1 GeV region.

In the S wave Argand plots of Fig. 4, a slow circular motion of the S wave amplitude is seen in the region from 0.80 GeV to 1.35 GeV. Above this mass, the S wave amplitude undergoes a very rapid circular motion with the greatest speed in the 1.420 GeV region. The precise mass of this maximum speed is clearly dependent on our choice of overall phase, as well as nonresonant S wave backgrounds. However, we believe any reasonable choice of phase will exhibit similar resonance behavior. Thus, we conclude that there exists an S wave resonance in this mass region, confirming the $0^+\kappa(1500)$ previously reported.[2)]

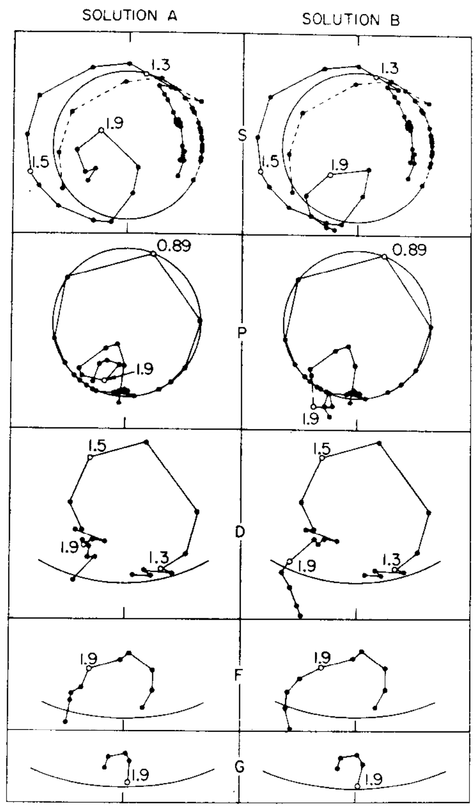

Fig. 4. Argand diagrams of the $K^-\pi^+$ elastic scattering partial waves for solutions A and B. The overall phase has been fixed as in Fig. 3.

In the mass region above 1.60 GeV circular motion is once again seen in the S wave Argand diagrams. Once again the details of this behavior are sensitive to the choice of overall phase, nonresonant backgrounds, as well as in this case, the particular solution being studied. However, all solutions display clear resonance loops at around 1900 MeV. We call this new state the $\kappa'(1900)$.

Figure 4 also shows resonance like behavior in the P wave near 1.65 GeV. Similar behavior was observed by Estabrooks et al. in two of four ambiguous solutions.[2] The precise interpretation of this structure is unclear. It is simplest to assume this behavior is due to a single resonance in the 1700 MeV region, and we will do when presenting parameters below. However, the rapid rise in the P wave amplitude in the 1600 MeV region combined with a very flat magnitude thereafter may indicate other structure in this region as well.

We have extracted resonance parameters for the leading states by fitting the rising edge of the associated partial wave magnitude to a relativistic Breit-Wigner resonance form with a Blatt-Weisskopf barrier factor.[5] In performing these fits, we have assumed that the turn-on of the partial waves associated with these states is resonance dominated. The resulting parameters are given in Table II. The resonance parameters obtained for the $4^+K^*(2090)$ were found to be independent of the solution fitted.

Faced with sizable nonresonant backgrounds, the overall phase uncertainty, and no clear theoretical understanding of the definition of resonance parameters, we have not attempted to determine the parameters of these underlying state precisely. Instead, we have estimated their parameters by ascribing circular motion to the Argand diagram resonance loops. The results are shown in Table II. Within the uncertainties of these estimates, the high mass S and P state parameters

TABLE II

LEADING RESONANCES			
J^P	Mass	Width	Elasticity
1^-	894.6 ± 0.8 MeV	49.8 ± 1.2 MeV	---
2^+	1428 ± 3 MeV	98 ± 8 MeV	0.43 ± 0.01
3^-	1753 + 25 MeV − 18 MeV	300 + 170 MeV − 80 MeV	0.16 ± 0.01
4^+	2070 + 100 MeV − 40 MeV	240 + 500 MeV − 100 MeV	0.07 ± 0.01
UNDERLYING RESONANCES			
J^P	Mass	Width	Elasticity
0^+	~ 1420 MeV	~ 240 MeV	~ 0.85
0^+	~ 1900 MeV	~ 230 MeV	~ 0.35 − 0.45
1^-	~ 1700 MeV	~ 200 MeV	~ 0.35

depend insignificantly on the particular solution chosen.

The resonance states observed in the $K^-\pi^+$ partial waves fit naturally into the framework expected from SU(3) and a simple $q\bar{q}$ quark model. The $K^*(892)$, $K^*(1430)$, $K^*(1780)$ and $K^*(2090)$ form an L-excitation ladder (with $q\bar{q}$ total spin $S = 1$) with L increasing from 0 to 3. The lower 0^+ state at ~1420 MeV is naturally classified as the lowest lying member of the $L = 1$, $S = 1$, $K^*(1430)$ triplet, while the higher 0^+ state can be naturally interpreted as the first radially excited recurrence of the 0^+, $L = 1$, $S = 1$ triplet member. The 1^- resonance behavior at 1700 MeV can be either the $L = 0$, $S = 1$ radial recurrence of the $K^*(892)$, the lowest lying member of the $L = 2$, $S = 1$, $K^*(1780)$ triplet, or perhaps both. Accurate measurements of this invariant mass region in inelastic decay channels should make it possible to establish which of these possibilities is the correct one.

REFERENCES

1. See: R. L. Kelly et al., Particle Data Group, Rev. Mod. Phys. 52, No. 2 (1980) and references therein.
2. P. Estabrooks et al., Nucl. Phys. B133, 490 (1978).
3. D. Aston et al., Phys. Lett. 99B, 503 (1981). Also see W. E. Cleland et al., Phys. Lett. 97B, 465 (1980).
4. E. Barrelet, Nuovo Cimento 8A, 331 (1972).
5. J. Blatt and V. Weisskopf, Theoretical Nuclear Physics, Wiley, New York (1952), p. 361, pp. 409-410.